The Tula uplift, northwestern China: Evidence for regional tectonism of the northern Tibetan Plateau during late Mesozoic–early Cenozoic time

Delores M. Robinson[†]
Guillaume Dupont-Nivet[‡]
George E. Gehrels[§]
Department of Geosciences, University of Arizona, Tucson, Arizona 85721, USA

Yueqiao Zhang
Institute of Geomechanics, Beijing 100081, People's Republic of China

ABSTRACT

Geologic mapping combined with petrographic and geochronologic studies in the Tula uplift of western China provides insights into the tectonic evolution of the northern edge of the Tibetan Plateau. The Mesozoic and early Cenozoic history of the area is preserved in the Tula uplift, which includes basin strata now exposed in a large syncline, pre-Mesozoic metamorphic basement, and Cretaceous plutons. Petrographic analyses of Upper Jurassic through Paleogene syntectonic sandstones show that rocks in the area were derived from lithologically diverse source terranes consisting of sedimentary, metasedimentary, and igneous rocks. These relationships imply that uplift in the Tula area began in Late Jurassic time and that uplift of the Tibetan Plateau's northern edge may have been initiated long before the early Tertiary India-Asia collision. Continued orogenic activity in the Tula area is recorded by intrusion of ca. 74 Ma granitoid bodies, latest Cretaceous to Paleogene shortening, uplift of Precambrian basement rock, the syntectonic nature of Cretaceous and Paleogene sandstones, and folding of all the basin strata into a regional north-vergent syncline. The northern range-bounding thrust of the Tula uplift has been recently active, suggesting that uplift and thickening continues in the northern Tibetan Plateau.

[†]E-mail: dmr@geo.arizona.edu.
[‡]E-mail: gdn@geo.arizona.edu.
[§]E-mail: ggehrels@geo.arizona.edu.

Keywords: Asian tectonics, China, syntectonic processes, Tibetan Plateau.

INTRODUCTION

Central Asia contains young mountain ranges, polycyclic basins filled with syntectonic sediments, and orogenic plateaus that are the result of progressive accretion of terranes and India onto the active southern margin of Asia (Şengör and Natal'in, 1996; Yin and Nie, 1996). Since about 1990, considerable geologic research in Asia has concentrated on Cenozoic deformation resulting from the Asia-India collision (see summaries in Matte et al., 1997; Yin and Harrison, 2000). The accretion of India created continental-scale features such as the Tibetan Plateau and the Altyn Tagh fault (Molnar and Tapponnier, 1975). This Cenozoic deformation overprinted earlier tectonic events, making it difficult to distinguish pre-Cenozoic deformation. In this paper, we explore the record of Mesozoic and early Cenozoic tectonism preserved within the Tula uplift in western China. This is the first comprehensive study in the Tula uplift, which is located in the northern part of the Arka Tagh in the remote north-central part of the Tibetan Plateau.

The Tula uplift is an ideal location in which to explore the history of Mesozoic and early Cenozoic tectonism, as the uplift has a nearly continuous stratigraphic section that was deposited during this time. By contrast, Mesozoic strata in most regions of central Asia have been removed by erosion or are buried by younger sediments (Graham et al., 1993). In previous studies, exposures around the edges of modern basins in Asia have been used to interpret the Mesozoic tectonic history (e.g., Watson et al., 1987; Graham et al., 1990; Hendrix et al., 1992, 1996; Carroll et al., 1995; Sobel, 1995, 1999; Sobel and Dimitru, 1997; Guo et al., 1998; Ritts, 1998; Yin, 1998; Vincent and Allen, 1999; Ritts and Biffi, 2000, 2001). In the Tula uplift, Upper Jurassic–Paleogene strata are exposed in a mountain range that has 2600 m of topographic relief. The Tula uplift includes the Tula syncline, which is a large regional fold within the Jurassic–Paleogene strata, metamorphic basement, and Cretaceous plutons. The uplift has had a protracted period of sedimentation and deformation that help address regional tectonic questions such as, Does the thickening recorded in the Tula area signify the beginning of Tibetan Plateau uplift? How much uplift of the Tibetan Plateau is pre-Himalayan? What was the paleogeographic setting of central Asia before Tertiary uplift of the plateau? How much of the deformation along the Altyn Tagh fault was inherited from pre-Tertiary orogenic events?

An additional objective of this research was to determine the origin of an oroclinal bend in the Tula uplift, which is apparent both from the topography of the present mountain range and from the pattern of units and contacts shown on the Geological Map of the Xinjiang Uygur Autonomous Region (Chen, 1985; 1:2,000,000) and the Regional Geology of Xinjiang Uyger Autonomous Region (XBGMR, 1993; 1:1,500,000). This feature, along with other arcuate mountain ranges in the region, may be a true orocline that formed as a result of distributed deformation

GSA Bulletin; January 2003; v. 115; no. 1; p. 000–000; 8 figures; 5 tables.

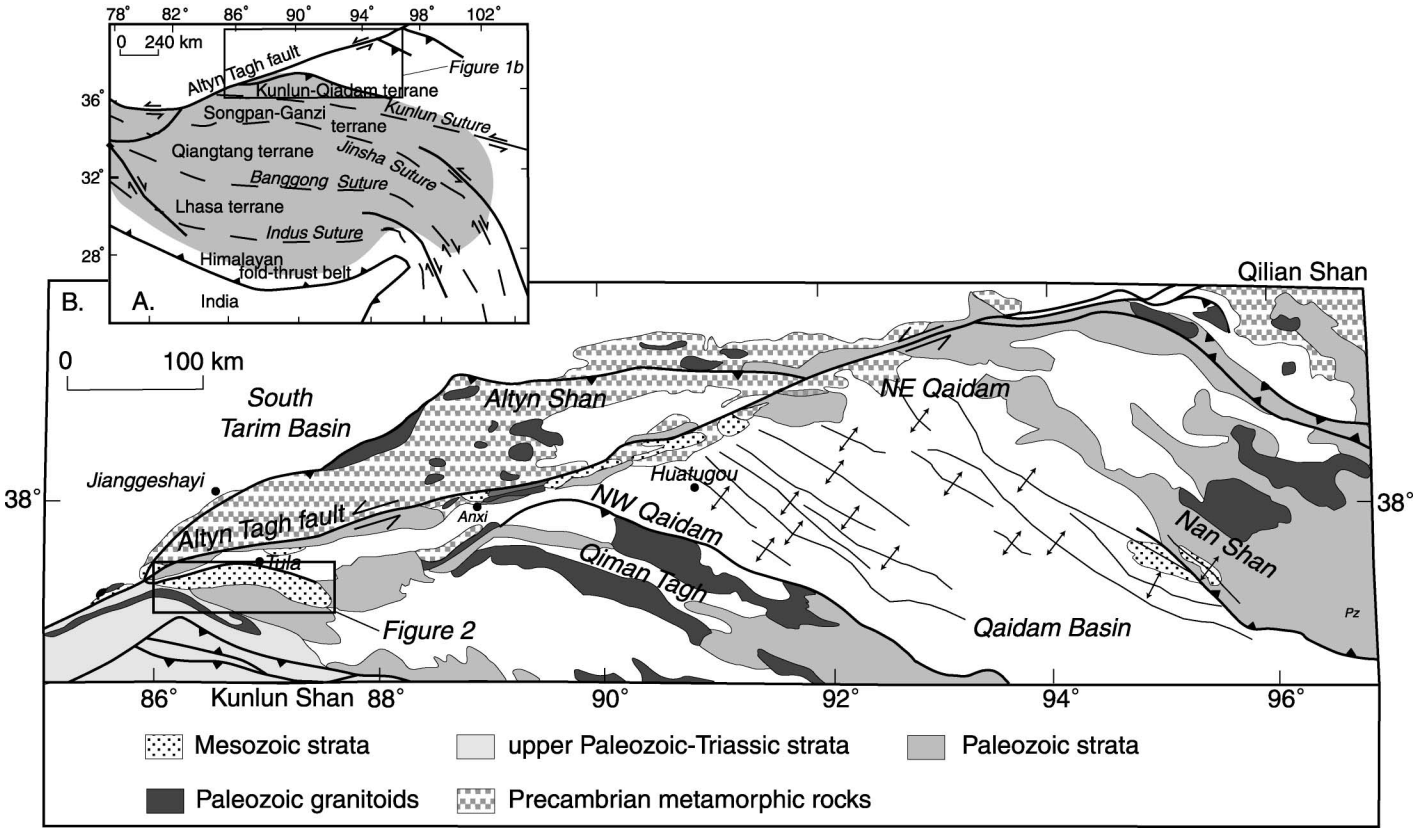

Figure 1. (A) Regional map of Asia showing the terranes, sutures, major faults, and major features. The Tibetan Plateau is highlighted in gray. The location of Figure 1B is shown with a rectangle. (B) Simplified geologic map of the central Altyn Tagh fault system (after A. Yin, unpublished). The location of Figure 2 is shown with a rectangle.

south of the Altyn Tagh fault (A. Yin, 1997, written commun.).

GEOLOGIC AND TECTONIC SETTING

The Tula uplift is located in the western part of the Kunlun-Qaidam terrane (Fig. 1A). Following is a summary of the terrane's Paleozoic and early Mesozoic tectonic history from Yin and Harrison (2000). The dominant feature of the Eastern Kunlun-Qaidam terrane is the Kunlun batholith (Harris et al., 1988; Jiang et al., 1992; Fig. 1B), which is part of a broad, early Paleozoic magmatic arc. The western part of the terrane consists of Middle to Late Proterozoic gneiss, schist, and marble. These lithologies are unconformably overlain by uppermost Proterozoic strata and Cambrian (?) to Middle Ordovician shallow-marine carbonate sequences (Fig. 1B). Between Late Ordovician and Mississippian (Early Carboniferous) time, volcanic deposits interbedded with marine strata were widespread in this region. Pennsylvanian (Upper Carboniferous) to Lower Permian sedimentary rocks are interbedded with abundant basalt, andesite, and rhyolite (Fig. 1B). The Kunlun batholith underwent another phase of intrusion in Late Permian to latest Triassic time.

The Mesozoic tectonic history of central Asia is dominated by accumulation of thick sequences of clastic strata, presumably in response to tectonic events along the convergent margin of southern Asia (Watson et al., 1987; Graham et al., 1988; Hendrix et al., 1992, 1996). The main accumulations of Mesozoic strata are in the Tula, Tarim, and Qaidam basins, which were intracontinental foreland basins in Late Jurassic and Cretaceous time (Ritts and Biffi, 2000). These basins remained centers of deposition throughout Mesozoic time (Graham et al., 1988). The Tula basin may have been continuous with the northwest Qaidam Basin (Ritts and Biffi, 2000). Both Xia (1990) and Ritts and Biffi (2001) have suggested that the Qaidam Basin formed during the amalgamation of Tibet by flexural response to contractional deformation. Xia (1990) viewed the source for the flexural load to be in the Kunlun Shan, whereas Ritts and Biffi (2001) proposed the load to be in the Qilian Shan. Mesozoic tectonism in central Asia may have also been influenced by the closure of the Mongol-Okhotsk Sea.

The western Tarim Basin is thought to be related to strike-slip motion between the Talas-Fergana (Burtman, 1980; Tseyeler et al., 1982) and Karakoram faults during Early Jurassic time (Sobel, 1999). In Late Jurassic and Cretaceous time, however, the western Tarim may have had a flexural origin as a foreland-style basin (Sobel, 1999).

The Cenozoic tectonic history of central Asia is dominated by strike-slip faulting caused by the Himalayan orogenic collision (Molnar and Tapponnier, 1975). The Altyn Tagh fault, one of the major continental-scale strike-slip faults in central Asia, is spatially separated from the Tula area by a Neogene–Quaternary intermontane basin (Fig. 1B). Motion along this >1200 km fault began during the Oligocene (Bally et al., 1986, Hanson, 1997; Rumelhart et al., 1997; Yin et al., 2002; Wang, 1997).

PRESENT STUDY

This paper documents the results of a reconnaissance-scale investigation into the

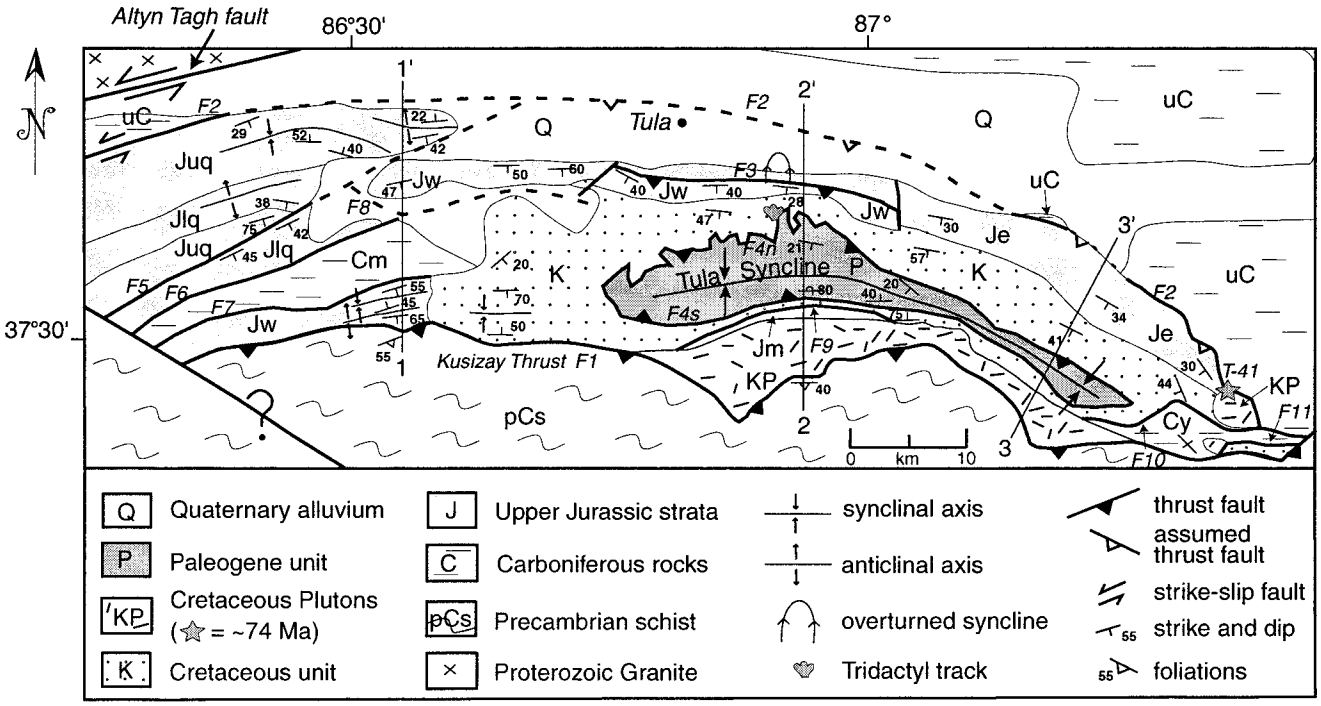

Figure 2. Geologic map of the Tula uplift showing stratigraphy, faults, and orientation as well as locations of cross sections depicted in Figure 6. Abbreviations: Jw—Upper Jurassic West Tula unit; Je—Upper Jurassic East Tula unit; Juq—Upper Jurassic upper Qarqan unit; Jlq—Upper Jurassic lower Qarqan unit; Jm—Upper Jurassic Muselik unit; Cy—Carboniferous Yak Valley unit; Cm—Carboniferous Mandalike unit; uC—Undivided Carboniferous rocks.

structural geology and stratigraphy of the Tula uplift. We conducted the work in reconnaissance fashion because of the remote nature of the study area. As a result, the structural data are ambiguous regarding the evidence for motion, displacement, and timing of the faults. We accessed most of the Tula uplift via a series of traverses over a period of two months. The extreme far-western region, the south-central region, and the extreme southeastern region were inaccessible. Mapping of the stratigraphy and structure was accomplished at a scale of 1:100,000, and samples were collected for petrographic and paleomagnetic analysis (see Dupont-Nivet et al., 2001).

Previous studies in the Tula area are limited. Geologic maps of the Xinjiang Uygur Autonomous Region (Chen, 1985; XBGMR, 1993) show an arcuate pattern of sedimentary rocks overlying Silurian and Carboniferous rocks in the Tula region. These maps suggest that faults separate Upper Jurassic and Carboniferous strata and that unconformities exist at the base of Cretaceous rocks and between Paleogene and underlying Cretaceous strata. Other studies in the Tula area include that of Guo et al. (1998), who reviewed the potential for oil exploration and the presence of oil- and asphalt-bearing sandstone in the Jurassic strata, and the description of mammal tracks from the Tula area (Ritts, 1998; Lockley et al., 1999).

Because the previous studies did not establish stratigraphic nomenclature for units in the Tula region, we use informal unit names. We have loosely divided the Upper Jurassic–Paleogene strata into seven units, from which we analyzed 30 standard petrographic thin sections of medium- to coarse-grained sandstone. This modal petrographic analysis of framework minerals enabled us to characterize units and to make preliminary assessments of provenance. Half of each thin section was stained for both calcic plagioclase and K-feldspar and point-counted (500 counts) by the same operator according to the Gazzi-Dickinson method, as described by Ingersoll et al. (1984).

Mapping in the Tula region enabled us to recognize several plutons south of the Tula uplift that had not been mapped previously. A sample from one of these plutons was collected for U-Pb geochronologic analyses. Zircons were separated from this sample by using standard separation procedures, and U-Pb ages were determined by isotope dilution–thermal-ionization mass spectrometry. All of the zircons analyzed were abraded to about two-thirds of their original diameter prior to dissolution and were analyzed as individual grains following the methods of Gehrels (2000).

STRATIGRAPHY

Mesozoic–Cenozoic strata in the Tula area rest unconformably on basement, which includes Precambrian, Ordovician, and Carboniferous rocks (Guo et al., 1998). Our mapping allows us to divide the Carboniferous rocks into three units, the Upper Jurassic strata into five units, and overlying strata into separate Cretaceous and Paleogene units. In the following sections, we describe the stratigraphy in more detail.

Pre-Jurassic Strata

Mesozoic strata in the Tula area unconformably overlie metamorphic rock, presumed to be Precambrian (Guo et al., 1998) (ps, Fig. 2), and undivided Carboniferous strata (uC). The Precambrian basement is composed of schist and gneiss with abundant quartz veins (Guo et al., 1998). Thin sections show a groundmass of quartz, biotite, and chlorite with porphyroblasts of plagioclase and perthitic feldspar ± muscovite, sphene, and zircon.

The undivided Carboniferous rock unit (uC, Fig. 2) is composed of green and red quartzite,

phyllite, and slate. The Yak Valley unit (Cy, Fig. 2) contains metamorphosed greenish quartzite with abundant quartz veins. Although Chen (1985) assigned a Late Jurassic age, this unit shares more characteristics, such as metamorphic grade and the abundance of greenish quartzite, with strata in the Tula area that are given a Carboniferous age. Thus, we assign the Yak Valley unit a Carboniferous age and estimate its thickness at 2 km. The Mandalike unit (Cm, Fig. 2) is a volcanic unit of uncertain age. Pyroclastic zones around its perimeter are fault bounded. Although Chen (1985) assigned it a Carboniferous age (Chen, 1985), Guo et al. (1998) reported that both Carboniferous pyroclastic rocks and Ordovician volcanic rocks are present in this region, and Pierce and Mei (1988) reported that volcanic rock is prevalent in Ordovician, Carboniferous, and Permian units of the area. Breccia in the pyroclastic zones ranges from centimeters to tens of meters in thickness. Small breccia fragments are composed of granitic fragments, quartzite, chert, sandstone, and siltstone. The maximum outcrop thickness of the Mandalike unit is 5 km.

Mesozoic–Lower Cenozoic Strata

Upper Jurassic Strata

The West Tula unit (Jw, Figs. 2 and 3, Table 1) crops out in the western and central Tula area and contains interbedded reddish and greenish sandstone, siltstone, and conglomerate beds (see Table 1 for a more complete description). The characteristic feature of this unit is thinly bedded reddish and greenish sandstone and siltstone horizons.

The East Tula unit (Je, Figs. 2 and 3, Table 1) crops out in the eastern part of the Tula uplift. Guo et al. (1998) assigned an early Late Jurassic age to strata in either the West or East Tula units (exact position of fossil locality is uncertain) on the basis of the presence of sporopollenin in dark mudstones. The East Tula unit is composed of conglomerate beds interbedded with variegated sandstone and siltstone beds. The presence of pink granite and greenish quartzite clasts in the upper part of the section is the distinguishing feature of this unit.

The lower Qarqan unit (Jlq, Figs. 2 and 3, Table 1) also crops out in the western part of the Tula uplift. It is separated by an unconformity from the overlying upper Qarqan unit. The lower Qarqan unit is isoclinally folded with beds of fine-grained sandstone, siltstone, sparry limestone, shale, and intercalated breccia beds. These breccia beds contain sandstone, siltstone, limestone, schist, and conglomerate and are the distinguishing features of this unit.

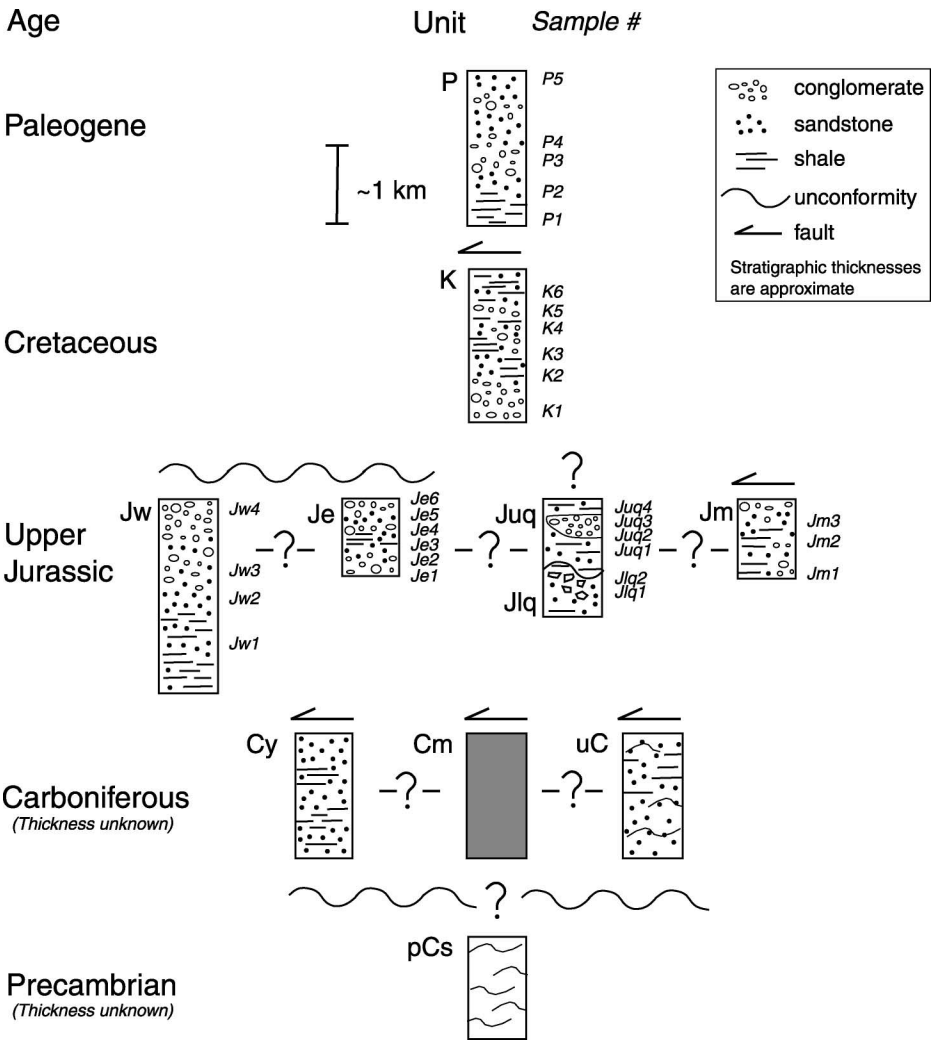

Figure 3. General stratigraphy of the Tula uplift. Note that the original relationships of the four Upper Jurassic sequences and the three Carboniferous sequences are uncertain. Unit abbreviations are the same as in Figure 2 with the addition of the following: P—Paleogene; K—Cretaceous; ps—Precambrian schist.

The upper Qarqan unit (Juq, Figs. 2 and 3, Table 1) crops out west of Tula and contains a thick section of conglomerate beds with clasts of chert and white and greenish quartzite punctuated by thin discontinuous beds of sandstone and siltstone. The unit's characteristic feature is the quartzite and chert conglomerate.

In the central Tula area, the Muselik unit (Jm, Figs. 2 and 3, Table 1) crops out south of the synclinal axis. The Muselik unit is a coarsening-upward section of sandstone and siltstone beds at the base and conglomerate beds at the top of the section. The strata's muted brown and tan color is its distinctive feature.

Stratigraphic Relationships of Jurassic Strata

The five Upper Jurassic units in the Tula syncline are distinguished on the basis of lithologic differences but are interpreted to be part of an Upper Jurassic clastic sequence. Figure 3 portrays our attempt to relate the different units to each other. In detail, however, specific age relationships of the various units are unclear, as our data do not provide any relative age control. The West Tula unit (Jw) in the western and central regions and the East Tula unit (Je) in the eastern region occupy the same structural position in the regional syncline and so may originally have been contiguous, in which case the stratigraphic differences noted may be the result of lateral facies changes within the basin. The nature of the

TABLE 1. LITHOLOGIC UNIT DESCRIPTIONS

Paleogene (P)
Structural thickness is ~1 km on south side of Tula syncline; basal contact—fault; upper contact—not preserved; section coarsens upward with an increase in the abundance of interbedded conglomerate, sandstone, and siltstone; clasts include quartzite, light colored gneiss, sandstone, siltstone, dolostone, and limestone; beds are tabular on a 10 m horizontal scale and lenticular at a larger scale; cliff-forming unit; trough cross-beds and ripples
Cretaceous (K)
Outcrop thickness on the north side of syncline is >3 km and <300 m on the south side (truncated by a fault); basal contact—angular unconformity with Jw and Je; upper contact—fault; section grades upward from 300 m of conglomerate into 2 km of red lenticular sandstone, siltstone, and shale with interspersed conglomerate beds, clasts are white, red,and green quartzite, tan and red siltstone, light gray and red sandstone, and rare metamorphic fragments; uppermost Km consists of interbedded conglomerate and sandstone; beds vary in thickness and are lenticular; trough cross-beds, soft-sediment deformation, mudcracks, ripple marks, and climbing ripples.
West Tula (Jw)
Monocline west of Tula contains ~1.5 km of continuous section, structural thickness is locally 2.5 km; base contact—covered by alluvium; upper contact—angular unconformity with overlying K; basal section contains ~1 km of interbedded gray to green sandstone and siltstone and grades into a thick sequence of interbedded conglomerate and green sandstone, above which are thinly bedded red siltstone, sandstone, and conglomerate beds; conglomerate beds are more common near the top of the section and have a dark green sandstone matrix; conglomerate clasts are 10 cm in diameter, rounded to subrounded, moderately well sorted clasts that include white quartzite, red plutonic rock, dark brown and orange weathering conglomerate, black volcanic rock, dark green and gray quartzite, maroon, dark gray, and green sandstone, and green and red siltstone; bedding in the sandstone and siltstone is lenticular on a 1 m scale; beds weather with a red stain; trough cross-beds, burrowed and rippled siltstone.
East Tula (Je)
Structural thickness of ~4 km but is faulted and folded; basal contact—covered by alluvium; upper contact—angular unconformity with overlying K; basal section contains green conglomerate interbedded with green, tan, and red siltstone and sandstone; clasts are subangular, moderately well sorted, and include green quartzite, light green phyllite, multicolored sandstone, and white vein quartz; overlying section is a brown to tan conglomerate and gray sandstone; top of the section has red sandstone, siltstone, and conglomerate with clasts of pink granite and green quartzite; yellowish sandstone and siltstone beds are common in the upper part of the section in the east; sandstone and siltstone beds are 1-m-thick lenticular beds; conglomerate beds are lenticular on a 10 m horizontal scale; channelized sandstone and siltstone beds, trough cross-beds and local paleosols.
Upper Qarqan (Juq)
Outcrop thickness of ~8 km, true thickness unknown; basal contact—unconformable with Jlq; upper contact—buried under alluvium or fault truncated; contains a thick section of resistant conglomerate that is well organized and well sorted; clasts include chert and white and green quartzite in a gray to green matrix; conglomerate beds are interbedded with thin black shales and green micaceous sandstone, siltstone, and shale; contains lenticular pods of conglomerate 3 m thick punctuated by thin lenticular beds of sandstone and siltstone.
Lower Qarqan (Jlq)
Isoclinally folded with an outcrop thickness of ~3 km; basal contact—bounded by a fault; upper contact—overlain unconformably by Juq; contains green to gray, fine-grained sandstone, green and tan fissile sandstone, sparry limestone, gray and red sandstone interbedded with light gray siltstone, thin black shale beds, and intercalated breccia beds <3 m thick; breccia contains a variety of lithologies including schist and conglomerate; bedding is lenticular over a 10 m horizontal scale; climbing ripples in siltstone.
Muselik (Jm)
Outcrop thickness of ~1 km; southern contact—intrusive; northern contact—fault; basal section has a coarse-grained tan and gray sandstone and beige and red siltstone, which grade upward into green conglomerate interbedded with brown sandstone on a 1 m scale; brown conglomerate at top of section contains clasts of chert, white quartzite, and variegated sandstone and siltstone; bedding is lenticular on a 10 m horizontal scale; trough cross-beds.

contact between the lower Qarqan (Jlq) and upper Qarqan (Juq) units varies; in one location, they are separated by a fault, whereas at another site, they are separated by an unconformity. The age relationship between the lower and upper Qarqan units and the West and East Tula units is uncertain. The Muselik unit (Jm) may be the same as the West or East Tula units, but is retained as a separate unit because it is fault bounded and has a distinctive brown and tan color. Petrographic data provide additional information that helps to further define the stratigraphy.

Cretaceous Strata

The Cretaceous unit (K, Figs. 2 and 3, Table 1) crops out in the central and eastern parts of the Tula syncline and is separated by a 12° angular unconformity from the underlying Upper Jurassic West and East Tula units. The Cretaceous unit is composed of generally fining-upward interbedded reddish sandstone and siltstone with thick conglomerate beds. The unit is intensely folded near the synclinal axis and dips gently at the northern edge of the Tula uplift. In the southeastern part of the Tula uplift, Cretaceous plutons intrude the Cretaceous strata, providing a minimum depositional age. Although a Cretaceous age is assigned to this unit by XBGMR (1993), Lockley et al. (1999) reported an Eocene age based on small tridactyl vertebrate tracks that appear to correlate with Eocene tracks found in North America. Two explanations for this inconsistency exist. It is possible that the track was derived from the youngest unit because it was discovered near the contact between the Cretaceous and Paleogene unit (Fig. 2), or the Cretaceous age assigned by XBGMR (1993) is actually Cretaceous through Eocene. Further investigation is needed to clarify the inconsistency in the available age data for this unit.

Paleogene Strata

In the central and eastern parts of the Tula syncline, the Paleogene unit (P, Figs. 2 and 3, Table 1) crops out in the core of the syncline. The Paleogene and Cretaceous units are separated by a thrust fault; thus, the original relationship is unknown. However, petrographic data suggest that the Paleogene unit was deposited in the Tula basin, overlying the Cretaceous unit. The fault that separates the Paleogene unit from the Cretaceous unit is the result of tight folding of the Tula syncline. Chinese researchers assigned a Paleogene age to these strata on the basis of the presence of Oligocene ostracods in the section (XBGMR, 1993). The section coarsens upward with an increase in the abundance of conglomerate toward the top. The characteristic feature is the dominance of limestone and metamorphic clasts in the conglomerate beds.

Cretaceous Plutons

Cretaceous plutons are located in the southern part of the Tula uplift and separate the basin strata from Precambrian metamorphic rocks to the south. The plutons are 2–6 km in diameter in the eastern and central regions and intrude the Upper Jurassic East Tula and Cretaceous units. In the western part of the Tula uplift, the intrusions are less abundant and too small to map at 1:100,000 scale. Samples collected from various granitic bodies are composed of quartz, K-feldspar, plagioclase, biotite, muscovite ± apatite, and zircon. The U-Pb age of the zircons from a granitic pluton is 74 ± 3 Ma (Table 2, Fig. 4; see star in Fig. 2).

TABLE 2. U-Pb ISOTOPIC DATA AND AGES FOR CRETACEOUS PLUTON

Grain mass (μg)	Apparent ages (Ma)					$^{207}Pb^*/^{235}U$	$^{207}Pb^*/^{206}Pb^*$
	Pb_c (pg)	U (ppm)	$^{206}Pb_m/^{204}Pb$	$^{206}Pb_c/^{208}Pb$	$^{206}Pb^*/^{238}U$		
13	1405	4148	52.5	1.2	88.9 ± 2.6	118.5 ± 16.7	762 ± 270
9	285	1462	57.9	1.3	86.2 ± 2.2	88.5 ± 14.1	149 ± 350
14	120	794	146.4	2.4	141.9 ± 1.4	145.1 ± 6.9	197 ± 100
12	205	949	119	2.1	178.2 ± 1.9	215.9 ± 1.2	650 ± 110
12	830	3028	63.2	1.4	103.9 ± 2.4	113.5 ± 14.9	319 ± 280
11	705	2421	46.3	1.1	74.5 ± 2.2	74.9 ± 17.6	88 ± 520
8	690	4738	90.5	1.8	133.2 ± 2.0	141.4 ± 11.7	281 ± 180
11	36	1256	307	4.1	74.9 ± 1.7	77.1 ± 3.8	143 ± 100
9	56	1804	234	3.5	74.7 ± 1.6	75.9 ± 4.9	116 ± 138
7	175	1652	118	2.3	151.8 ± 1.8	159.3 ± 9.5	273 ± 130

Notes: All analyses are of single zircon crystals. $^{206}Pb/^{204}Pb$ is measured ratio, uncorrected for blank, spike, or fractionation. $^{206}Pb/^{208}Pb$ is corrected for blank, spike, and fractionation. Most concentrations have an uncertainty of 25% due to uncertainty in mass of grain. Constants used: $^{238}U/^{235}U = 137.88$. Decay constant for $^{235}U = 9.8485 \times 10^{-10}$. Decay constant for $^{238}U = 1.55125 \times 10^{-10}$. All uncertainties are at the 95% confidence level. Pb blank was ~5 pg. U blank was <1 pg. All analyses conducted by using conventional isotope dilution and thermal-ionization mass spectrometry, as described by Gehrels (2000).

*Radiogenic Pb.

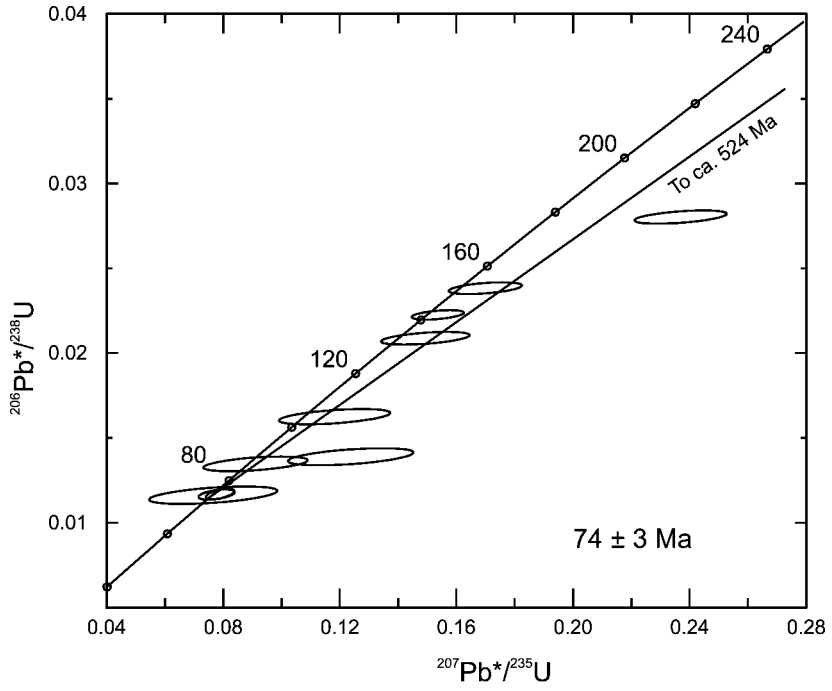

Figure 4. U-Pb single-zircon analyses ($n = 10$) from a Cretaceous pluton. The interpreted age of 74 ± 3 Ma (95% confidence level) is based on three concordant analyses.

PETROGRAPHIC DATA

Results

We point counted 19 samples from Upper Jurassic strata, 6 from Cretaceous strata, and 5 from Paleogene rocks. Definitions of the parameters counted are shown in Table 3, and the recalculated data, average modes, and standard deviations are shown in Table 4. We display our results by using framework-grain assemblages (QtFL, QmFLt), framework mineral grains (QmPK), and framework lithic grains (QpLvtLsm).

Generally, all samples, except those from the upper Qarqan unit, are litharenites and cluster together in QtFL, QmFLt, and QmPK space (Fig. 5). The upper Qarqan unit is a lithofeldspathic arenite and plots distinctly away from the other units. In ternary QtFL space, all framework-grain compositions reside near the quartz pole, except for the upper Qarqan unit. Because many of the quartzose grains are polycrystalline quartzite and quartzose tectonites, the cluster shifts to the lithics pole in QmFLt space.

Quartz Fraction

The average modes of the West Tula, East Tula, lower Qarqan, Muselik, Cretaceous, and Paleogene units are grouped because they plot similarly in ternary space (Figs. 5B and 5D). These units have little feldspar and a high percentage of total quartz grains (average %QtFL = 75,15,10), resulting from abundant polycrystalline (Qp) and foliated polycrystalline (Qpt) quartzite (Table 4). The upper Qarqan unit has a low percentage of total quartz grains and a moderate amount of feldspar (%QtFL = 57,30,13). The lower Qarqan and Paleogene units have lower percentages of monocrystalline quartz (Qm) than the West Tula, East Tula, or Muselik units (QmFLt). The monomineralic populations in all the samples except the upper Qarqan unit are dominated by monocrystalline quartz and plagioclase (%QmPK = 66,27,7). The upper Qarqan unit has a lower percentage of monocrystalline quartz and subequal plagioclase and potassium feldspar contents (%QmPK = 25,40,35), suggesting its source included metamorphic and sedimentary and a plutonic rock.

Lithic Fraction

All units have high total lithic and low feldspar contents (average %QmFLt = 27,14,59), except for the upper Qarqan unit that has a moderate amount of feldspar and low monocrystalline quartz content (%QmFLt = 10,29,61). A high lithic fraction is indicative of syntectonic sediments. The lithic fraction in all the samples is dominated by sedimentary and metasedimentary grains (Figs. 5C and 5D) and is represented by foliated polycrystalline quartzite grains, chert, limestone, siltstone, shale, phyllite, and schist. Volcanic lithic fragments are moderately abundant (up to ~18%) in a few samples (Table 4).

Petrographic Relationships

Although the original stratigraphic relationships of the various Upper Jurassic units are unknown because most units are fault bounded, the petrographic data provide some insights. The point counts of the West and East Tula units are very similar and as mentioned previously, these two units occupy the same structural position in the syncline. Although the West and East Tula units are lithologically somewhat different, this may be the result of lateral facies changes, and the two units may originally have been contiguous. Two samples from the lower Qarqan unit are completely different from one another, suggesting that we

TABLE 3. PETROGRAPHIC PARAMETERS

Qm	Monocrystalline quartz
Qp	Polycrystalline quartz
Qpt	Foliated polycrystalline quartz
Qss	Monocrystalline quartz in sandstone/quartzite lithic grain
C	Chert
Qt	Total quartzose grains (= Qm + Qp + Qpt + Qss + C)
K	Potassium feldspar (including perthite, myrmekite, microcline)
P	Plagioclase feldspar (including Na and Ca varieties)
F	Total feldspar grains (= K + P)
Lvl	Lath-work volcanic grains
Lvm	Microlitic volcanic grains
Lvf	Felsic volcanic grains
Lvv	Vitric volcanic grains
Lvt	Total volcanic lithic grains (= Lvl + Lvm + Lvf + Lvv)
Lph	Phyllite
Lsch	Schist
Lma	Marble (foliated, coarse-grained)
Lshs	Mudstone and siltstone
Lls	Limestone
Ld	Dolostone
Lsm	Total metasedimentary lithic grains (= Lshs + Lph + Lsch + Lma + Lls + Ld)
Ls	Total sedimentary lithic grains (= Lshs + Lls + Ld)
Lm	Total metamorphic lithic grains (= Lph + Lsch + Lma)
L	Lithic grains (= Lvt + Lsm)
Lt	Total lithic grains (= Qp + Qpt +Qss + C + Lvt + Lsm)
M	Phyllosilicates = muscovite, biotite, chlorite, kaolinite
D	Dense minerals = apatite, amphibole, tourmaline, zircon, sphene

do not have enough data to characterize this unit. Petrographically, the upper Qarqan unit is distinct from the other units in the Tula area. The average modes of the Cretaceous and Upper Jurassic Muselik units are indistinguishable in all the ternary diagrams (Fig. 5). Although the Muselik unit was assigned a Jurassic age, because it is fault bounded and has unique lithologies, it may be Cretaceous in age. Further work is necessary to clarify this relationship.

Provenance Interpretations

The sedimentary strata in the Tula uplift are very immature and have a high proportion of unstable lithics and feldspars. All of the samples plot within or near the recycled-orogen provenance field of Dickinson (1985) (Fig. 5A). Sandstones that plot within this field are typical of foreland basins and texturally and compositionally immature sediments derived from nearby tectonically active highlands. Thus, all units are undoubtedly syntectonic and were derived from a local source that was lithologically diverse, consisting of metamorphic, igneous, and metasedimentary rocks. The fact that the Upper Jurassic units are syntectonic suggests that uplift on the northern part of the Tibetan Plateau began in Late Jurassic time, concurrent with tectonic activity on the southern margin of Asia. The syntectonic nature of the Cretaceous and Paleogene units suggests that uplift continued through Cretaceous and early Tertiary time in the Tula area.

Paleocurrent data collected >300 km to the east by Ritts (1998) suggests that the source of the Upper Jurassic and Cretaceous strata in the northwestern Qaidam Basin was located to the north. However, current directions in the Tula uplift are potentially different than those in the northwest Qaidam Basin. Thus, the source area is ambiguous. If sediment in the Tula area came from the north, any potential source terranes for the Mesozoic strata are at present far from Tula because of the 400 km of offset (Ritts and Biffi, 2000) on the Altyn Tagh fault just north of the Tula area. The source area would now be located in the western Kunlun Shan, which contains a multitude of Phanerozoic sedimentary rocks and Paleozoic–Mesozoic igneous bodies (Sobel, 1999). However, if the source of the Upper Jurassic and Cretaceous rock is located to the south, the strata may have been derived from the pre-Mesozoic metamorphic basement. The source of the volcanic lithics could be the unroofing of the Kunlun arc to the south. Additional petrographic analyses coupled with statistically significant paleocurrent data would help resolve the provenance of the Upper Jurassic and Cretaceous Tula basin sedimentary rocks. Our mapping suggests that the Paleogene strata were derived from the Precambrian basement rock south of the Tula syncline, and the petrographic data are concordant with that suggestion.

STRUCTURAL GEOLOGY

Tula Syncline

The Tula uplift is bounded by Precambrian basement to the south, Carboniferous rocks to the east, and the active Altyn Tagh fault to the north (Fig. 2). Upper Jurassic through Paleogene strata are folded into a north-verging syncline that has steep dips on its south limb and moderate to shallow dips on its north limb. Upper Jurassic and Cretaceous strata south of the syncline are bounded by faults. The synclinal axis and strata in the central part have an east strike, whereas strata in the eastern region have a northwest strike. This bend in the trace of the fold between the east and central regions gives the Tula uplift its arcuate shape.

Kuzisay Thrust

The Kuzisay thrust (Fig. 2, F1 in Table 5) is a south-dipping regional-scale thrust fault that carries Precambrian metamorphic basement in its hanging wall. In the area of cross section 1–1′ (Fig. 6), the footwall of the Kuzisay thrust is the Upper Jurassic West Tula unit. Near cross section 2–2′, the footwall is the Upper Jurassic Muselik unit, and near cross section 3–3′ it is the Cretaceous unit and Carboniferous Yak Valley unit. The fault clearly cuts rocks of Late Jurassic age in the western part of the Tula syncline and dips ~50° to the south on the basis of the orientation of foliation measurements near the fault. Cretaceous plutons separate the Kuzisay thrust from sedimentary strata in the central and eastern areas. Erosional patterns between the Precambrian basement rock and the Cretaceous plutons suggest that the Kuzisay thrust cuts the plutons.

Other Thrust Faults (See Table 5)

The Tula uplift is bounded to the north by a thrust fault (F2 in Table 5, Fig. 6). At one locality in the eastern region, this range-bounding thrust fault places the East Tula unit over the undivided Carboniferous basement. Recent activity on this range-bounding thrust fault is shown by offset Quaternary gravels in the central part of the Tula uplift. In the western part of the Tula uplift, the fault has a near-vertical trace and subhorizontal slickenlines that suggest a significant component of oblique slip (Fig. 6A). Thus, F2 may be influenced by the proximity of the Altyn Tagh fault. Farther to the west, F2 joins, is cut by, or traces very close to the Altyn Tagh fault.

An intraformational thrust fault (F3, Table 5, Fig. 6B) occurs within the West Tula unit in the central region of the Tula uplift. Thrust fault F3 created an overturned syncline in the West Tula unit, strikes N90°W, and dips 50°SW (Fig. 7).

TABLE 4. RECALCULATED DATA

Sample	Qt	Qm	F	L	Lt	Qm	P	K	Qp	Lvt	Lsm	Lm	Lvt	Ls	M†	D†
Jw1	68	26	13	18	61	66	30	5	52	4	44	51	9	41	4	1
Jw2	74	34	12	14	54	73	20	6	54	5	6	43	14	43	3	0
Jw3	72	36	13	15	51	74	22	5	56	6	38	48	10	42	3	0
Jw4	65	34	18	16	48	65	27	8	52	3	45	40	7	53	6	1
avg.	70	32	14	16	54	69	25	6	54	5	33	45	10	45		
s.d.	4	5	3	2	5	5	5	2	2	1	18	5	3	6		
Je1	71	30	15	14	55	66	21	13	43	18	29	37	49	14	1	1
Je2	73	31	21	6	47	59	28	12	71	0	29	58	0	42	6	0
Je3	79	38	15	7	47	72	10	18	79	1	20	40	7	53	0	0
Je4	77	31	14	9	56	69	26	6	72	1	27	43	5	52	1	0
Je5	75	45	11	15	44	81	13	6	47	3	50	43	6	51	1	2
Je6	69	37	12	18	51	75	12	13	37	6	57	48	10	42	9	0
avg.	74	35	15	11	50	70	18	11	58	7	35	45	13	43		
s.d.	4	6	4	5	5	8	8	5	18	11	15	7	18	15		
Juq1	58	11	32	10	58	25	25	50	75	3	22	58	13	29	5	3
Juq2	56	9	31	13	60	22	56	22	69	11	19	43	38	20	20	0
Juq3	56	13	25	19	62	35	50	15	58	5	37	78	12	10	22	4
Juq4	59	7	31	10	62	18	30	52	79	1	20	89	7	4	10	0
avg.	57	10	29	13	61	25	40	35	70	5	25	67	17	16		
s.d.	1	3	3	4	2	7	15	19	9	4	8	21	14	11		
Jlq1	85	24	5	10	72	83	17	0	78	4	18	58	58	26	1	3
Jlq2	62	16	26	13	58	39	30	30	55	18	27	32	32	29	3	1
avg.	74	20	15	11	65	61	24	15	67	11	23	45	45	27		
s.d.	17	5	15	2	10	31	9	22	16	10	6	18	18	2		
Jm1	75	37	16	9	47	69	31	0	69	6	25	18	21	62	1	3
Jm2	73	19	19	8	63	50	50	0	80	8	11	31	43	26	2	0
Jm3	92	26	3	5	71	91	9	0	88	2	10	50	17	33	2	0
avg.	80	27	13	7	60	70	30	0	79	5	15	33	27	40		
s.d.	10	9	9	2	12	20	20	0	10	3	8	16	14	19		
K1	78	39	12	9	49	76	24	0	67	7	26	43	21	36	6	0
K2	87	25	6	7	69	81	16	4	84	8	8	12	52	36	2	1
K3	80	26	15	5	59	63	37	0	88	2	10	62	14	24	2	1
K4	78	26	15	7	58	63	25	11	85	2	13	33	13	53	2	5
K5	67	28	20	12	51	58	42	0	65	7	28	49	20	31	3	1
K6	75	29	17	8	54	64	36	0	78	3	19	71	12	18	8	2
avg.	78	29	14	8	57	68	30	2	78	5	17	45	22	33		
s.d.	6	5	5	3	7	9	10	5	10	3	8	21	15	12		
P1	77	17	15	8	68	54	24	22	80	5	15	32	24	45	2	0
P2	74	27	20	7	53	58	32	10	80	0	20	55	0	45	5	0
P3	68	22	16	16	62	57	35	8	60	2	38	51	4	45	13	2
P4	71	14	20	9	67	41	59	0	79	3	18	55	14	31	7	0
P5	74	38	13	13	50	75	24	1	56	8	36	48	18	34	11	2
avg.	73	24	17	11	60	57	35	8	71	4	25	48	12	40		
s.d.	4	9	3	4	8	12	14	9	12	3	11	10	10	7		

Notes: avg.—average; s.d.—standard deviation. Recalculated data is normalized within each group (QtFL, QmFLt, QmPK, QpLvtLsm, QpLvtLsm, LmLvtLs) and listed as a percentage.
†Raw data not normalized.

The fault between the Paleogene strata and the underlying deformed Cretaceous unit is interpreted to be an out-of-the-syncline thrust fault (F4n and F4s, Table 5). Because the Paleogene strata have petrographic characteristics similar to those of the other units in the Tula syncline (see Petrographic Data), we suggest that this unit was deposited in the Tula basin and not transported into the basin by a fault. Kinematic indicators beneath F4n in the Cretaceous unit indicate a reverse fault and are evidence for the out-of-syncline thrust fault, which accommodated room problems resulting from tight folding of the Tula syncline. F4s on the southern limb of the Tula syncline has a near-vertical orientation with an east strike (Figs. 6B and 6C). On the northern limb, F4n has an orientation of N87°E, 20°SE and has an unknown sense of slip.

Other Faults

Because of the reconnaissance nature of this study, we were unable to determine the sense of slip and magnitude of offset for most faults in the study area (Table 5). Stratigraphic units in the western region are bounded by faults (including F5, F6, F7, and F8), but the nature of the faults is unclear (Fig. 6A). F9 is located south of the Tula syncline in the central region (Fig. 6B) and may be a strike-slip or thrust fault. F10 and F11 are located in the extreme southeastern region (Fig. 2) and strike generally east, with an unknown sense of slip. The sense of motion for all these faults was interpreted from map relationships, slickenlines, and stratigraphic offset. Slickenlines on some of the faults in the western Tula area are subhorizontal, indicating strike-slip, but the sense of slip is ambiguous. Further analyses would help resolve these structural problems.

TECTONIC HISTORY

Tula Uplift

The earliest record of Mesozoic tectonic history of the Tula area begins with the deposition of Upper Jurassic strata (West Tula, East Tula, upper Qarqan, lower Qarqan, and Muselik units) (Fig. 8A). Stratigraphic relationships and petrographic data are not sufficient to document the primary relationships between the various Upper Jurassic units, but we have operated on the assumption that all of the units were laterally contiguous and part of the same basin sequence. The source for this thick sequence of clastic strata is unclear. The similarity of metamorphic clasts in the Upper Jurassic strata with Precambrian basement rocks south of the Kuzisay thrust raises the possibility that the source was to the south, and that the Kuzisay thrust was active during Late Jurassic time. Ritts (1998), however, collected paleocurrent data from the northwest Qaidam Basin, >300 km east of Tula, and concluded that clastic material flowed into the basin from the north during Late Jurassic time. A systematic collection of paleocurrent data in the Tula area would more accurately locate the source.

After deposition, the Upper Jurassic units were deformed (Fig. 8B) in Early Cretaceous time. In the west, the Carboniferous Mandalike unit has been placed by faults F6 and F7 between the Upper Jurassic lower Qarqan and West Tula units. If a layer-cake stratigraphy is assumed, then motion on these faults and related deformation of the Upper Jurassic units must have occurred before deposition of Cretaceous strata because the Cretaceous strata are not offset. An angular unconformity is present at the base of the Cretaceous section (Fig. 8C), which suggests that the Jurassic strata were uplifted, tilted, and eroded prior to the deposition of the overlying Cretaceous strata. The nature of this deformational event is also uncertain—local relationships are consistent with early motion along the Kuzisay thrust and uplift to the south.

In Late Cretaceous time, plutons intruded and northward motion occurred along the Kuzisay thrust (Fig. 8D). The Kuzisay thrust uplifted the Precambrian schist and caused widespread deformation in footwall Upper Jurassic and Cretaceous units. The paucity of metamorphic clasts in the Cretaceous unit indicates that the main phase of uplift of the Precam-

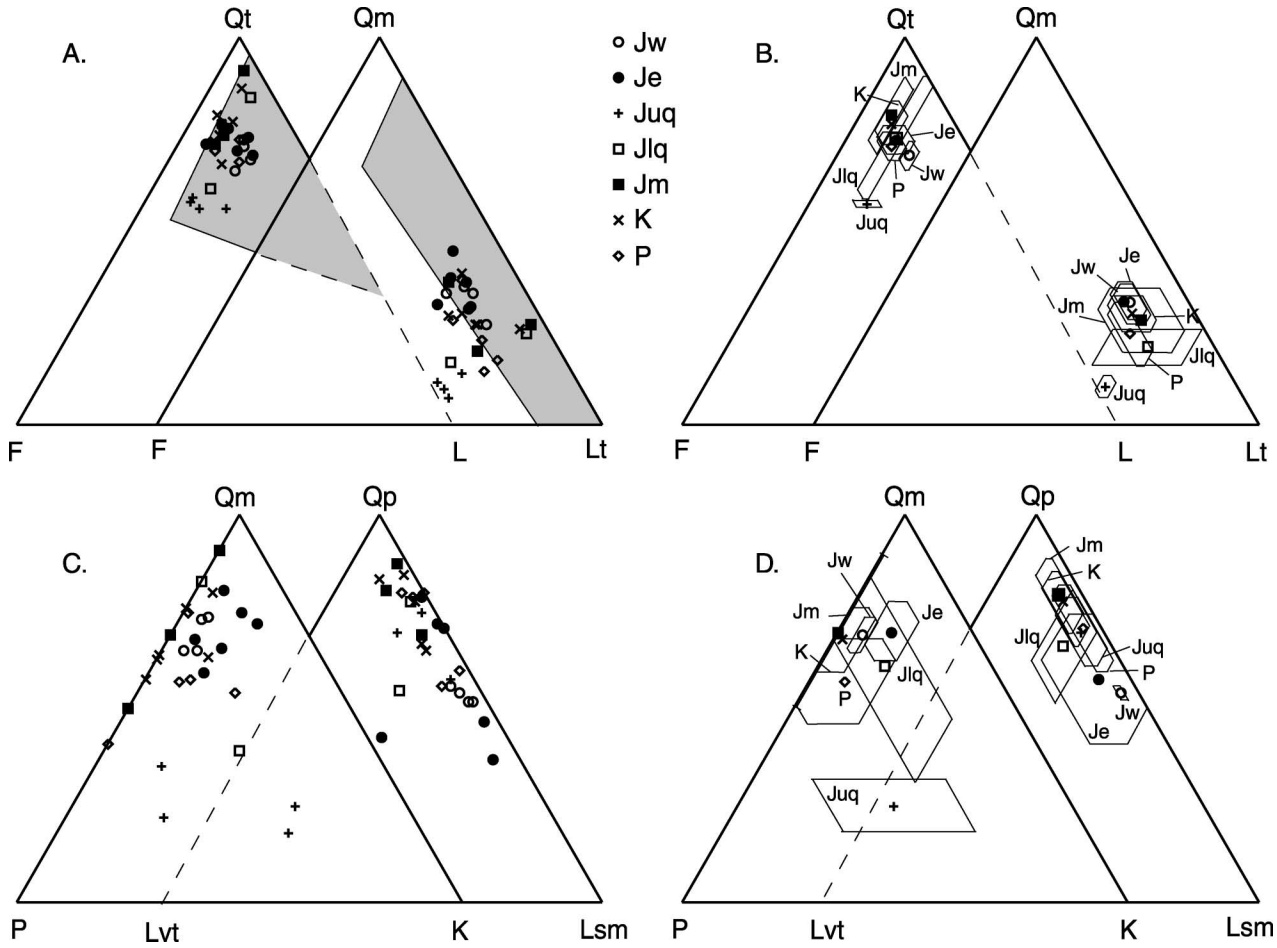

Figure 5. Ternary diagrams for Upper Jurassic–Paleogene strata in the Tula uplift: (A) QtFL and QmFLt diagrams with each sample depicted by a symbol; the recycled-orogen provenance fields from Dickinson (1985) are shown by the light gray shading. (B) QtFL and QmFLt diagrams; average modes for each unit are depicted by a single symbol; standard deviations are depicted by trapezoids surrounding each symbol. (C) QmPK and QpLvtLsm diagrams with each sample depicted by a symbol. (D) QmPK and QpLvtLsm diagrams showing average modes for each unit by a single symbol; the standard deviations are shown by the surrounding trapezoids.

TABLE 5. FAULT DATA

Fault	Region	Structural data	Type of fault
F1	All regions	Precambrian basement over West Tula unit, N70°E, 45–65°S	Thrust
F2	All regions	Western—upper Qarqan next to undivided Carboniferous, near vertical	Thrust or strike-slip
		Central—deformed Quaternary gravels	Thrust
		Eastern—East Tula next to undivided Carboniferous, near vertical	Thrust or strike-slip
F3	Central	Intraformational; N90°W, 50°S	Thrust
F4n	Central and eastern	Paleogene over Cretaceous; Cretaceous deformed under fault; N70°E, 20–30°S	Thrust
F4s	Central and eastern	Paleogene over Cretaceous; N90°E, 75°N to 80°S overturned	Thrust or strike-slip
F5	Western	Upper Qarqan on top of lower Qarqan, E-W, 70°N; upper Qarqan and West Tula, relationship uncertain, covered by Quaternary	Thrust or strike-slip
F6	Western	Lower Qarqan over Mandalike, N55°E, 40°SE; dike intruded along contact in one location	Probably thrust
F7	Western	Mandalike over West Tula, N80°W, 80°N; zone of deformation	Probably thrust
F8	Western	Separates lower Qarqan from West Tula; assumed buried under Quaternary inferred to strike NW-SE	Unknown
F9	Central	Cretaceous next to Muselik; N90°E, vertical	Probably strike-slip possibly thrust
F10	Eastern	Cretaceous next to Yak Valley; vertical, various orientations	Unknown
F11	Eastern	Yak Valley next to Cretaceous; contact inferred	Assumed

brian schist occurred after deposition of the Cretaceous strata.

The Paleogene unit, however, contains abundant metamorphic, plutonic, and metasedimentary clasts that probably originated from the hanging wall of the Kuzisay thrust. Their presence suggests that uplift of rocks to the south was occurring along the fault, causing the development of flexural accommodation space, into which Paleogene strata were deposited (Fig. 8E). The lack of penetrative deformation in the Paleogene unit but abun-

dant deformation in the Cretaceous and Upper Jurassic units also suggests that thrusting ended just prior to deposition of Paleogene strata.

After or during deposition of the Paleogene strata, the entire basin was folded into a syncline (Fig. 8F). The northward asymmetry of the syncline suggests that contractional deformation originated from the south. We interpret this folding to have occurred in response to reactivation or continued motion along the Kuzisay thrust. It is possible that the Kuzisay thrust roots into a basal décollement and that motion on a ramp-anticline buried to the south of the syncline that ties into the system could have caused the overturning of the south limb of the Tula syncline and fed slip northward into the northern range-bounding thrust fault (F2). In either case, the tight folding caused an out-of-the-syncline thrust fault (F4) between the Paleogene unit and underlying Cretaceous strata.

Faulting in post-Paleogene time caused further deformation of rocks in the Tula uplift (Fig. 8G). Deformed Quaternary gravels in the northern part of the Tula syncline indicate that the range-bounding thrust fault (F2) is currently active. We suggest that motion along the Kuzisay thrust has occurred since Paleogene time, creating the northern range-bounding thrust fault (F2), the intraformational thrust in the West Tula unit (F3), and the overturned syncline.

The arcuate bend in the Tula syncline occurred after formation of the syncline because the synclinal axis and the Paleogene strata are also bent. This event was probably synchronous with motion that created the range-bounding thrust fault because the fault is also bent. Unfortunately, our mapping in the Tula area did not enable us to determine whether this arcuate bend is related to the nearby Altyn Tagh fault.

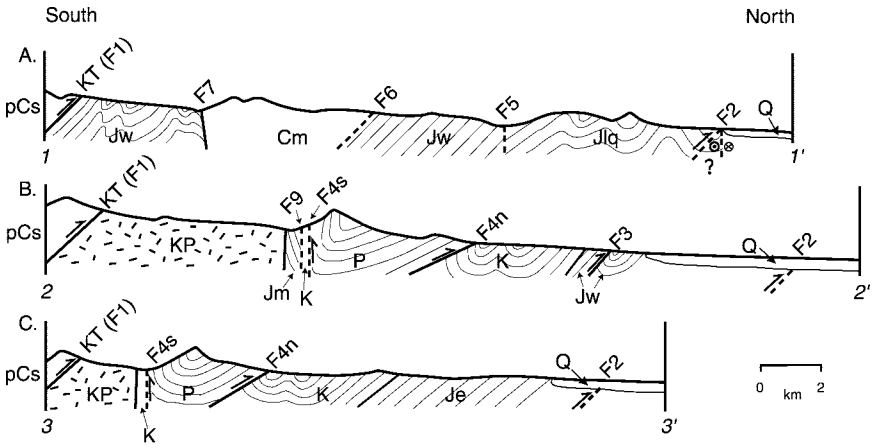

Figure 6. Three scaled cross sections across the Tula uplift. The locations of cross-section lines and unit abbreviations are shown in Figure 2. The nomenclature of the faults is shown in Table 5.

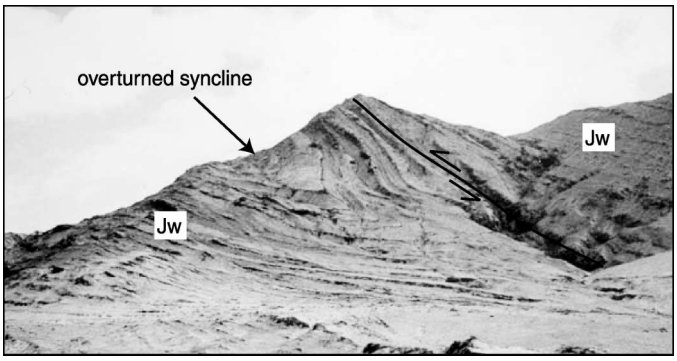

Figure 7. Photograph of an overturned syncline in the Upper Jurassic West Tula unit; fold is attributed to regional folding of basin strata into the Tula uplift. Field of view covers ~500 m.

Regional Synthesis

According to previous syntheses, the Mesozoic basins of central Asia formed in response to tectonic activity on the southern edge of Asia (Watson et al., 1987; Graham et al., 1988; Hendrix et al., 1992, 1996). Stratigraphic and structural relationships in the Tula area strongly support this view, as outlined in the following.

The Qiangtang terrane accreted onto the Kunlun-Qaidam and Songpan-Ganzi terranes along the Jinsha suture in Triassic–Early Jurassic time (Coward et al., 1988; Matte et al., 1996; Kapp et al., 2000; Wang et al., 2000; Jolivet et al., 2001). It is possible that this collision created the accommodation space into which the Upper Jurassic strata were deposited. In the north and west Tarim Basins, a major influx of conglomerate occurred in Late Jurassic time followed by rapid subsidence that is attributed to the accretion of the Qiangtang block (Hendrix et al., 1992; Sobel, 1995). Regional uplift during Early to Middle Jurassic time is confirmed in the northwest Qaidam Basin by $^{40}Ar/^{39}Ar$ dating and apatite fission-track analysis that show that the region underwent ~100–150 °C of cooling (Sobel et al., 2001). Possible sources for uplift and deformation and resulting creation of accommodation space include Qiangtang terrane collision along the Jinsha suture and Lhasa terrane collision along the Banggong suture (Coward et al., 1988; Wang et al., 2000). Collision of the Lhasa terrane may also have caused the deposition of the Upper Jurassic strata, but the exact timing of collision remains undefined. Deformation of the Upper Jurassic strata in the Tula basin may also be related to this event. Transport of detritus into the Tula basin and accumulation of the Cretaceous strata are probably a direct result of the Lhasa collision. However, Ritts (1998) noted an increase in basin-subsidence rates during Jurassic and Early Cretaceous time and concluded that subsidence occurred mainly in response to a sustained contractional setting rather than in response to specific collisions.

The Cretaceous plutons were emplaced at ca. 74 Ma. Erosional patterns suggest that motion occurred on the Kuzisay thrust shortly thereafter placing Precambrian rock over strata in the Tula basin. Because these crustal-thickening events occurred >500 km from the trench in a retro-arc setting, the origin and magma source of the plutons and the cause of the basement uplift are enigmatic. They may be related to late-stage emplacement of the Kunlun arc. It is interesting that this pluton- and basement-cored uplift is similar in style and distance from the plate boundary to the

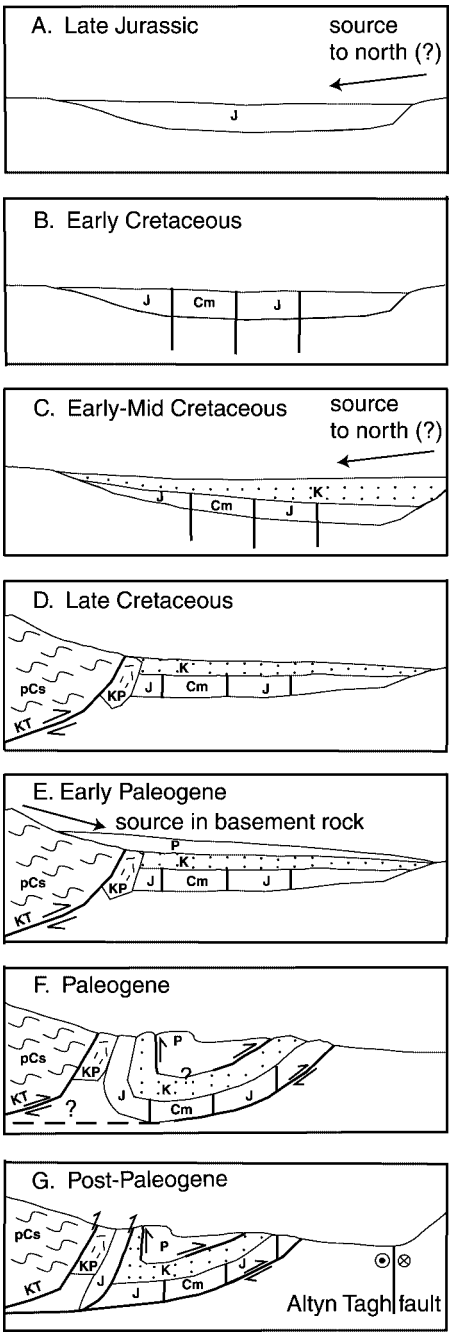

Figure 8. Schematic cross sections portraying the evolution of the Tula uplift. South is to the left in each diagram. (A) Deposition of Upper Jurassic strata. (B) Faulting of Upper Jurassic strata, but with an unknown sense of motion on the faults. (C) Deposition of Lower to middle Cretaceous strata of the Cretaceous unit. (D) Intrusion of Cretaceous plutons followed by motion on the Kuzisay thrust in Late Cretaceous time. (E) Subsequent deposition of the Paleogene strata in early Paleogene time. (F) Folding of the strata in the Tula area into a syncline during and/or after Paleogene time; faults between the Paleogene and Cretaceous units may or may not be connected at depth. (G) Faulting and uplift of the present range that continues to the present time.

Laramide basement uplifts in western North America. The emplacement of these plutons may have been the result of flat-slab accreting of one of the accreting terranes. Emergence of the basement south of the Tula syncline along the Kuzisay thrust records crustal thickening in Paleogene time and may be a local manifestation of regional uplift of the northern Tibetan Plateau.

The dominant cause of uplift of the Tibetan Plateau and of the large strike-slip faults in the Asian interior (e.g., Altyn Tagh fault) is the accretion of India onto the southern margin of the Lhasa terrane, which began in early Cenozoic time. Yet, the syntectonic nature of the sandstones in the Tula area, the uplift of basement rock, and the injection of plutons argue that some uplift and thickening along the northern part of the Tibetan Plateau occurred at least since ca. 74 Ma and maybe since Late Jurassic time. If the events in the Tula area are related to the regional uplift of the Tibetan Plateau, uplift of the plateau may have commenced significantly earlier then most previous models suggest. A widespread view is that uplift of the Tibetan Plateau occurred during Cenozoic time (e.g., Peltzer and Tapponnier, 1988; Burchfiel and Royden, 1991; Yin et al., 2002), but pre-Cenozoic crustal shortening is also supported by Sobel et al. (2001), who documented 100 °C of Late Jurassic cooling in the northwest Qaidam area, and Murphy et al. (1997), who suggested significant that crustal thickening occurred in the Lhasa terrane during the Cretaceous.

The accumulation of a thick Paleogene clastic wedge records the main phase of crustal thickening in the region. Deformation along the Kuzisay fault, which created the accommodation space, may have been kinematically linked to the Altyn Tagh fault, much as thrust faults in the Nan Shan feed displacement into the Altyn Tagh fault today (Burchfiel et al., 1989). The similarity in timing between deposition of Paleogene strata and uplift of the basement terrane to the south of the Tula uplift support a linkage to the initiation of motion along the Altyn Tagh fault during Oligocene time (Bally et al., 1986; Hanson, 1997; Rumelhart et al., 1997; Wang, 1997). Alternatively, uplift of the basement along the Kuzisay thrust may have been completely decoupled from the kinematics of the Altyn Tagh fault. Subsequently, the Tula basin was folded into a north-verging syncline, and the modern boundaries of the Tula syncline were created by motion on the Kuzisay thrust to the south and on the range-bounding fault to the north. This deformation may or may not have been related to the Altyn Tagh fault.

The axial bend in the east-central region of the Tula syncline gives the structure its arcuate map pattern (Fig. 2). Three prominent hypotheses exist for the formation of the bend. The first involves distributed left-lateral motion along the Altyn Tagh fault that may have sheared the rocks south of the fault, creating an oroclinal bend (Yin and Harrison, 2000). The second hypothesis is that the bend results from the intersection of lateral and frontal ramps along the front of the Tula uplift, where the apparent bend in the eastern region occurs (Yin and Harrison, 2000). We propose that a third hypothesis—involving a decrease in slip to the east and west along the range-bounding thrust, creating a thrust salient—is also a possibility. All of these options are consistent with data obtained through field mapping. Paleomagnetic studies (Dupont-Nivet et al., 2001), however, show that the sediments of the Tula uplift have not been rotated about a vertical axis, and, thus, only the second and third hypotheses are viable. The arcuate nature of the Tula uplift therefore is probably not genetically related to displacement along the Altyn Tagh fault. Studies of other arcuate features that exist northeastward along the Altyn Tagh fault may help to evaluate the feasibility of the second and third hypotheses. Detailed mapping in these arcuate structures may find the presence of a frontal ramp as required in the second hypothesis. Although the possibility remains that some deformation within the Tula uplift may be kinematically related to the Altyn Tagh fault, the Tula uplift could have formed entirely independently of the continental-scale strike-slip fault. This alternative suggests that the deformation along the Altyn Tagh fault in this area may be restricted to within a few tens of kilometers of the fault.

CONCLUSIONS

Field investigations in the Tula uplift along the northern margin of the Tibetan Plateau provide a clearer understanding of Mesozoic and Cenozoic tectonics in central Asia. Mesozoic–Cenozoic strata within the uplift provide a rare glimpse into the protracted tectonic history of the region. Our investigations have revealed the following:

1. The lithic composition of Upper Jurassic sandstones and the deformation, uplift, and erosion of Upper Jurassic strata suggest that significant regional uplift occurred in the Tula area during Late Jurassic time. This uplift may have been caused by accretion of the Qiangtang or Lhasa terranes onto the southern margin of Asia.

2. The intrusion of Cretaceous plutons and the uplift of basement rock along the Kuzisay thrust support crustal thickening and shortening in the northern Tibetan Plateau prior to deposition of Paleogene strata, and perhaps beginning by ca. 74 Ma. The intrusion and uplift may record collisional tectonics along the southern margin of Asia during or prior to the onset of the Indian collision.

3. Folding of the Tula syncline is syn- or post-Paleogene and is probably related to continued motion on the Kuzisay thrust.

4. A prominent bend in the synclinal axis developed after the Tula syncline was formed, giving the structure its arcuate shape. Field relationships do not discriminate between several possible hypotheses for the formation of the Tula syncline. However, paleomagnetic data (Dupont-Nivet et al., 2001) rule out the possibility that it is the result of shear along the Altyn Tagh fault. Thus, the oroclinal shape may result from either a salient of a south-dipping thrust or the intersection of a frontal ramp with a lateral ramp.

5. The Tula uplift has an active northern range-bounding fault, which suggests that thickening and uplift of the Tibetan Plateau is still occurring. These data and other studies suggest that this region has a long history related to the tectonic activity occurring synchronously on the southern margin of Asia.

6. Uplift in the northern Tibetan Plateau may have begun in Late Jurassic time, continued through Cretaceous and early Tertiary time, and continues to the present day. Therefore, the northern Tibetan Plateau may have been tectonically active—and undergoing regional compressional deformation, uplift, and erosion—long before the early Tertiary India-Asia collision. Further stratigraphic, provenance, and geochronologic investigations in the Tula syncline will clarify the details of this tectonic activity.

ACKNOWLEDGMENTS

We thank Wang Xiao Feng and the Institute of Geomechanics, Beijing, PRC, for organizing our field logistics in China. E. Cowgill and An Yin provided assistance within China and perceptive discussions. P. DeCelles provided invaluable assistance with the petrographic and sedimentological data. We also thank An Yin as the leader of the Altyn Tagh fault project. Formal reviews by Ed Sobel and an unknown reviewer improved this manuscript. A. Hanson, O. Pearson, B. Ritts, Ed Sobel, and An Yin provided informal reviews in the earliest stages of this manuscript. This study was supported by National Science Foundation Continental Dynamics Program grant EAR-9725663.

REFERENCES CITED

Bally, A.W., Chou, I.M., Clayton, R., Eugster, H.P., Kidwell, S., Meckel, L.D., Ryder, R.T., Watts, A.B., and Wilson, A.A., 1986, Notes on sedimentary basins in China—Report of the American Sedimentary Basins Delegation to the People's Republic of China: U.S. Geological Survey Open-File Report 86–327, 108 p.

Burchfiel, B.C., and Royden, L.H., 1991, Tectonics of Asia 50 yr after the death of Emile Argand: Eclogae Geologica Helvetica, v. 84, p. 599–629.

Burchfiel, B.C., Deng, Q., Molnar, P., Royden, L., Qang, Y., Zhang, P., and Zhang, W., 1989, Intracrustal detachment within zones of continental deformation: Geology, v. 17, p. 448–452.

Burtman, V.S., 1980, Faults of middle Asia: American Journal of Science, v. 280, p. 725–744.

Carroll, A.R., Graham, S.A., Hendrix, M.S., Ying, D., and Zhou, D., 1995, Late Paleozoic tectonic amalgamation of northwestern China: Sedimentary record of the northern Tarim, northwestern Turpan, and southern Junggar Basins: Geological Society of America Bulletin, v. 107, p. 571–594.

Chen, Z., ed., 1985, Geological map of Xinjiang Uygur Autonomous Region, China: Beijing, Geological Publishing House, scale 1:2,000,000.

Coward, M.P., Kidd, W.S.F., Pan, Y., and Shackleton, R.M., 1988, Structure of the 1985 Geotraverse, Lhasa to Golmud: Royal Society of London Philosophical Transactions, Ser. A, v. 327, p. 307–336.

Dickinson, W.R., 1985, Interpreting provenance relations from detrital modes of sandstones, *in* Zuffa, G.G., ed., Provenance of arenites: Dordrecht, Netherlands, Reidel, p. 333–361.

Dupont-Nivet, G., Butler, R.F., Yin, A., Robinson, D.M., Zhang, Y., and Qiao, W.S., 2001, Paleomagnetism of the Altyn Tagh South of the Altyn Tagh Fault: Implications for Intracontinental Deformation Processes in Asia: EOS Transactions AGU, Fall Meeting Supplement Abstract T12F–06, v. 82, no. 47.

Gehrels, G.E., 2000, Introduction to detrital zircon studies of Paleozoic and Triassic strata in western Nevada and northern California, *in* Soreghan, M.J., and Gehrels, G.E., eds., Paleozoic and Triassic paleogeography and tectonics of western Nevada and northern California: Geological Society of America Special Paper 347, p. 1–17.

Graham, S.A., Zuchang, X., Carroll, A., Mcknight, C., 1988, Mesozoic–Cenozoic basins of western China as example of partitioned retro-arc foreland basin system: Association of American Petroleum Geologists Bulletin, v. 72, p. 191.

Graham, S.A., Brassell, S., Carroll, A.R., Xiao, X., Demaison, G., McKnight, C.L., Liang, Y., Chu, J., and Hendrix, M.S., 1990, Characteristics of selected petroleum source rocks, Xianjiang Uygur Autonomous Region, northwest China: American Association of Petroleum Geologists Bulletin, v. 74, p. 493–512.

Graham, S.A., Hendrix, M.S., Wang, L.B., and Carroll, A.R., 1993, Collisional successor basins of western China: Impact of tectonic inheritance on sand composition: Geological Society of America Bulletin, v. 105, p. 323–344.

Guo, Z., Zhang, Z., and Zeng, F., 1998, Discovery of megathick oil sandstone and asphalt in the Jurassic System in the Tula basin and its significance: Chinese Science Bulletin, v. 43, p. 1898–1901.

Hanson, A.D., 1997, Evidence of Cenozoic erosional unroofing adjacent to the northern Qaidam Basin, northwest China, preserved within basin-margin strata: Geological Society of America Abstracts with Programs, v. 29, no. 6, p. A143.

Harris, N.B.W., Xu, R., Lewis, C.L., Haekeworth, C.J., Zhang, Y., 1988, Isotopic geochemistry of the 1985 Tibet Geotraverse, Lhasa to Golmud: Royal Society of London Philosophical Transactions, Ser. A, v. 327, p. 263–85.

Hendrix, M.S., Graham, S.A., Carroll, A.R., Sobel, E.R., McKnight, C.L., Schulein, B.S., and Wang, Z., 1992, Sedimentary record and climatic implications of recurrent deformation in the Tian Shan: Evidence from Mesozoic strata of the north Tarim, south Junggar and Turpan Basins, northwest China: Geological Society of America Bulletin, v. 104, p. 53–79.

Hendrix, M.S., Graham, S.A., Amory, J.Y., and Badarch, G., 1996, Noyon Uul syncline, southern Mongolia: Lower Mesozoic sedimentary record of the tectonic amalgamation of central Asia: Geological Society of America Bulletin, v. 108, p. 1256–1274.

Ingersoll, R.V., Bullard, T.F., Ford, R.L., Grimm, J.P., Pickle, J.D., and Sares, S.W., 1984, The effect of grain size on detrital modes: A test of the Gazzi-Dickinson point-counting method: Journal of Sedimentary Petrology, v. 54, p. 103–116.

Jiang, C., Yang, J., Feng, B., Zhu, Z., Zhao, M., et al., 1992, Opening-closing tectonics of Kunlun Mountains, Beijing: Geologic Publishing House, 224 p. (in Chinese with English abstract).

Jolivet, M., Brunel, M., Seward, D., Xu, Z., Yang, J., Roger, F., Tapponnier, P., Malavieille, J., Arnaud, N., and Wu, C., 2001, Mesozoic and Cenozoic tectonics of the northern edge of the Tibetan Plateau: Fission-track constraints: Tectonophysics, v. 343, p. 111–134.

Kapp, P., Yin, A., Manning, C.E., Murphy, M., Harrison, T.M., Spurlin, M., Ding, L., Deng, X.-G., and Wu, C.-M., 2000, Blueschist-bearing metamorphic core complexes in the Qiangtang block reveal deep crustal structure of northern Tibet: Geology, v. 28, p. 19–22.

Lockley, M.G., Ritts, B.D., and Leonardi, G., 1999, Mammal track assemblages from the early Tertiary of China, Peru, Europe, and North America: Palaios, v. 14, p. 398–404.

Matte, Ph., Tapponnier, P., Arnaud, N., Bourjot, L., Avouac, J.P., Vidal, P., Liu, Q., Pan, Y.S., and Wang, Y., 1996, Tectonics of western Tibet, between the Tarim and the Indus: Earth and Planetary Science Letters, v. 142, p. 311–330.

Matte, Ph., Mattauer, M., Olivet, J.M., and Griot, D.A., 1997, Continental subductions beneath Tibet and the Himalayan orogeny: A review: Terra Nova, v. 9, p. 264–270.

Molnar, P., and Tapponnier, P., 1975, Cenozoic tectonics of Asia: Effects of a continental collision: Science, v. 189, p. 419–426.

Murphy, M.A., Yin, A., Harrison, T.M., Durr, S.B., and Chen, Z., 1997, Significant crustal shortening in south-central Tibet prior to the Indo-Asian collision: Geology, v. 25, p. 719–722.

Peltzer, G., and Tapponnier, P., 1988, Formation and evolution of strike-slip faults, rifts, and basins during the India-Asia collision: An experimental approach: Journal of Geophysical Research, v. 93, p. 15,085–15,117.

Pierce, J.A., and Mei, H., 1988, Volcanic rocks of the 1985 Tibet Geotraverse Lhasa to Golmud: Royal Society of London Philosophical Transactions, Ser. A, v. 327, p. 203–213.

Ritts, B.D., 1998, Mesozoic tectonics and sedimentation, and petroleum systems of the Qaidam and Tarim Basins, northwest China [Ph.D. thesis]: Stanford, California, Stanford University, 691 p.

Ritts, B.D., and Biffi, U., 2000, Magnitude of post–Middle Jurassic (Bajocian) displacement on the central Altyn Tagh fault system, northwest China: Geological Society of America Bulletin, v. 112, p. 61–74.

Ritts, B.D., and Biffi, U., 2001, Mesozoic northeast Qaidam Basin: Response to contractional reactivation of the Qilian Shan, and implications for the extent of Mesozoic intracontinental deformation in central Asia, *in* Hendrix, M.S., and Davis, G.A., eds., Paleozoic and Mesozoic tectonic evolution of central Asia: From continental assembly to intracontinental deformation: Geological Society of America Memoir 194, p. 293–316.

Rumelhart, P.E., 1998, Cenozoic basin evolution of southern Tarim, northwestern China: Implications for the

uplift history of the Tibetan Plateau [Ph.D. thesis]: Los Angeles, University of California, 298 p.

Rumelhart, P.E., Yin, A., Butler, R., Richards, D., Wang, X., Zhou, X., and Zhang, Q., 1997, Oligocene initiation of deformation of northern Tibet, evidence from the Tarim Basin, northwest China: Geological Society of America Abstracts with Programs, v. 29, no. 6, p. A143.

Şengör, A.M.C., and Natal'in, B.A., 1996, Paleotectonics of Asia: Fragments of a synthesis, *in* Yin, A., and Harrison, T.M., eds., The tectonics of Asia: New York, Cambridge University Press, p. 486–640.

Sobel, E.R., 1995, Basin analysis and apatite fission-track thermochronology of the Jurassic–Paleogene southwest Tarim Basin, northwest China [Ph.D. thesis]: Stanford, California, Stanford University, 308 p.

Sobel, E.R., 1999, Basin analysis of the Jurassic–Lower Cretaceous southwest Tarim Basin, northwest China: Geological Society of America Bulletin, v. 111, p. 709–724.

Sobel, E.R., and Dimitru, T.A., 1997, Exhumation of the margins of the western Tarim Basin during the Himalayan orogeny: Journal of Geophysical Research, v. 102, p. 5043–5064.

Sobel, E.R., Arnaud, N., Jolivet, M., Ritts, B.D., and Brunel, M., 2001, Jurassic to Cenozoic exhumation history of the Altyn Tagh range, northwest China, constrained by $^{40}Ar/^{39}Ar$ and apatite fission track thermochronology, *in* Hendrix, M.S., and Davis, G.A., eds., Paleozoic and Mesozoic tectonic evolution of central Asia: From continental assembly to intracontinental deformation: Geological Society of America Memoir 194, p. 247–267.

Tseyeler, V.M., Florenskiy, V.S., Vasyukov, V.S., and Turov, A.V., 1982, Tectonic structure of the northern Fergana Range: International Geology Review, v. 24, p. 881–890.

Vincent, S.J., and Allen, M.B., 1999, Evolution of the Minle and Chaoshui Basins, China: Implications for Mesozoic strike-slip basin formation in central Asia: Geological Society of America Bulletin, v. 111, p. 725–742.

Wang, E., 1997, Displacement and timing along the northern strand of the Altyn Tagh fault zone, northern Tibet: Earth and Planetary Science Letters, v. 150, p. 55–64.

Wang, X., Metcalfe, I., Jian, P., He, L., and Wang, C., 2000, The Jinshajiang-Ailaoshan suture zone, China: Tectonostratigraphy, age and evolution: Journal of Asian Earth Sciences, v. 18, p. 675–690.

Watson, M.P., Hayward, A.B., Parkinson, D.N., and Zhang, Zh.M., 1987, Plate tectonic history, basin development and petroleum source rock deposition onshore China: Marine Petroleum Geology, v. 4, p. 205–225.

XBGMR (Bureau of Geology and Mineral Resources of Xinjiang Uygur Autonomous Region), 1993, Regional geology of Xinjiang Uygur Autonomous Region: Beijing, Geological Publishing House, Geological Memoirs, Series 1, Number 32, 841 p., scale 1:1,500,000.

Xia, B., 1990, Terranes of Xizang (Tibet), China, *in* Wiley, T.J., Howell, D.G., and Wong, F.L., eds., Terrane analysis of China and the Pacific rim: Circum-Pacific Council for Energy and Mineral Resources Earth Science Series, v. 13, p. 231–241.

Yin, A., and Harrison, T.M., 2000, Geologic evolution of the Himalayan-Tibetan orogen: Annual Review of Earth and Planetary Science, v. 28, p. 211–280.

Yin, A., and Nie, S.Y., 1996, A Phanerozoic palinspastic reconstruction of China and its neighboring regions, *in* Yin, A., and Harrison, T.M., eds., The tectonics of Asia: New York, Cambridge University Press, p. 442–485.

Yin, A., Rumelhart, P.E., Butler, R., Cowgill, E., Harrison, T.M., Foster, D.A., Ingersoll, R.V., Zhang Qing, Zhou Xian-Qiang, Wang Xiao-Feng, Hanson, A., and Raza, A., 2002, The uplift history of the Tibetan Plateau as recorded in the Cenozoic stratigraphy of southern Tarim, northwestern China: Geological Society of America, v. 114, p. 1257–1295.

MANUSCRIPT RECEIVED BY THE SOCIETY 24 AUGUST 2001
REVISED MANUSCRIPT RECEIVED 18 APRIL 2002
MANUSCRIPT ACCEPTED 7 MAY 2002

Printed in the USA